Journal of Theoretical Biology 271 (2011) 1–9

Contents lists available at ScienceDirect

Journal of Theoretical Biology

journal homepage: www.elsevier.com/locate/yjtbi

Outbreak properties of epidemic models: The roles of temporal forcing and stochasticity on pathogen invasion dynamics

Paul E. Parham [a,*], Edwin Michael [b]

[a] Grantham Institute for Climate Change, Department of Infectious Disease Epidemiology, Imperial College London, St. Mary's Campus, Praed Street, London W2 1PG, UK
[b] Department of Infectious Disease Epidemiology, Imperial College London, St. Mary's Campus, Praed Street, London W2 1PG, UK

ARTICLE INFO

Article history:
Received 18 May 2010
Received in revised form
7 September 2010
Accepted 8 November 2010
Available online 19 November 2010

Keywords:
Master equations
Temporal variability
Infectious disease modelling
Invasion

ABSTRACT

Despite temporally forced transmission driving many infectious diseases, analytical insight into its role when combined with stochastic disease processes and non-linear transmission has received little attention. During disease outbreaks, however, the absence of saturation effects early on in well-mixed populations mean that epidemic models may be linearised and we can calculate outbreak properties, including the effects of temporal forcing on fade-out, disease emergence and system dynamics, via analysis of the associated master equations. The approach is illustrated for the unforced and forced SIR and SEIR epidemic models. We demonstrate that in unforced models, initial conditions (and any uncertainty therein) play a stronger role in driving outbreak properties than the basic reproduction number R_0, while the same properties are highly sensitive to small amplitude temporal forcing, particularly when R_0 is small. Although illustrated for the SIR and SEIR models, the master equation framework may be applied to more realistic models, although analytical intractability scales rapidly with increasing system dimensionality. One application of these methods is obtaining a better understanding of the rate at which vector-borne and waterborne infectious diseases invade new regions given variability in environmental drivers, a particularly important question when addressing potential shifts in the global distribution and intensity of infectious diseases under climate change.

1. Introduction

Many infectious and non-infectious diseases demonstrate strong seasonal patterns in prevalence, with transmission of climatically dependent infectious diseases, such as malaria, only possible during limited periods of the year in many locations (typically influenced by temperature or rainfall characteristics (Craig et al., 1999)). Childhood diseases such as measles have also been recognised as forced by the nature of the school year, with the significantly higher contact rates during term times, when combined with other drivers of measles, shown to lead to the recurrent cyclical nature of incidence data (Keeling and Grenfell, 2002; Conlan and Grenfell, 2007). More generally, four key mechanisms have been identified as potential causes of seasonality in infectious disease systems in reviews elsewhere (Altizer et al., 2006; Grassly and Fraser, 2006), which in the context of climate-driven vector-borne diseases may be summarised as (a) changing contact patterns or behaviours (e.g. biting rates, human migration/movement patterns, vector dispersal), (b) changing environmental conditions (e.g. affecting biting rates, vector survival and the duration of parasite lifecycles), (c) fluctuations in demographic rates and intermediate host population dynamics (e.g. mosquitoes, snails and ticks) and (d) changes in underlying host immunity continuing to replenish the pool of susceptibles. It is also clear that such mechanisms may drive system dynamics on a range of timescales from hourly to long-term inter-annual variability and influences from mechanisms such as El Niño-Southern Oscillation (ENSO).

The inclusion of such mechanisms in infectious disease models also affects our interpretation of fundamental epidemiological concepts such as the basic reproduction number R_0, which needs to account for when infection is introduced, as this may strongly influence outbreak properties such as the likelihood of invasion, real-time growth rate and fade-out. Such considerations are closely linked with decisions regarding the timing and choice of suitable intervention strategies given local biological and environmental conditions (Grassly and Fraser, 2006), which clearly will also be important for guiding the design of adaptation strategies against vector-borne microparasitic infections, such as malaria, as a result of climate change (Ruiz et al., 2008).

Realistic mathematical models of infectious disease transmission, in general, reside on the edge of analytical tractability due to non-linearity in the transmission process, with even the simplest deterministic transmission model, namely the SIR model developed by

* Corresponding author. Tel.: +44 20 7594 3266.
E-mail address: paul.parham@imperial.ac.uk (P.E. Parham).

0022-5193/$ - see front matter © 2010 Elsevier Ltd. All rights reserved.
doi:10.1016/j.jtbi.2010.11.015

Kermack and McKendrick (1927), only approximately solvable. Thus, it is clear that the additional inclusion of temporal forcing in transmission models only serves to further complicate our understanding and despite approximate results on the behaviour of such models (Dietz, 1976), generic and rigorous analytical methods are currently lacking (Keeling and Rohani, 2007), although some theoretical research has recently emerged on the derivation of the basic reproduction number and epidemic growth rate in seasonally forced systems (Bacaër, 2007; Bacaër and Ouifki, 2007).

Furthermore, the analysis of temporally forced non-linear epidemic models within stochastic frameworks has received little attention to date due to the complexity of the problem, despite representing the most realistic framework for capturing the behaviour of many intrinsically or extrinsically forced infectious diseases. However, for infections in the early stages of emergence in homogeneous populations, the lack of population immunity or the small fraction of infected individuals means that the non-linear effect of saturation can be neglected and the problem reduces to a temporally forced linear stochastic system. Thus, we make the implicit general assumption here that temporal forcing in transmission takes place on shorter timescales than disease outbreak dynamics, which allows us to illustrate more transparently the theoretical framework incorporating the effects of stochasticity and seasonality, as well as highlighting key analytical insights. We note, however, that this assumption is likely to be most relevant to understanding the dynamics of seasonal infectious diseases with either small basic reproduction numbers, long generation times or both, as well as infections (particularly vector-borne diseases) strongly driven by changes in environmental or climatic variables, though it is worth noting that the linearising assumption is, in general, unlikely to hold over the entire duration of temporal changes in transmission.

Here, we begin analysis of this problem by developing and using the framework of master equations to better understand the dynamics of infectious disease outbreaks in this regime, an issue often of paramount public-health importance in assessing the speed, timing and intensity at which intervention measures should be introduced to control spread. The use of master equations, whereby the probability of occurrence of each possible disease state is simultaneously considered, to understand the behaviour of stochastic infectious disease models has been described elsewhere (Keeling and Ross, 2008), along with applications to epidemic processes in homogeneous models (Chen and Bokka, 2005) and structured/hierarchical models (Grabowski and Kosinski, 2004; Rozhnova and Nunes, 2009), yet by comparison to their deterministic counterparts, relatively little infection modelling work has adopted such methods. The approach has, however, been used to address specific questions such as the prospects for control and elimination of onchocerciasis in Africa (Duerr and Eichner, 2010), coevolution in ecological communities (Dieckmann and Law, 1996), the dynamics of systems with competing strains of varying pathogenicity (Stollenwerk and Jansen, 2003), stochastic metapopulation dynamics (Alonso and McKane, 2002), the role of immunity in small livestock populations on transmission dynamics (Viet and Medley, 2006) and the effect of density-dependence and time-varying susceptibility on plant disease dynamics (Stollenwerk and Briggs, 2000). A key outcome of the method is that irrespective of the complexities and non-linearities involved in the transmission dynamics, this approach is linear and thus allows ready analytical insights into the behaviour and process dynamics of stochastic systems.

Given that SIR and SEIR compartmental approaches continue to form the basis of many infectious disease models of microparasites, we analyse the effect of variability in transmission on the outbreak properties of both, but emphasise that the approach may be equivalently applied to higher dimensional systems typical of more complex or realistic models. In particular, we suggest that such modelling frameworks will represent an important advance for facilitating a more realistic understanding of how predicted climate change may govern the invasion properties of vector-borne microparasitic diseases into newly at-risk populations.

2. The unforced SIR model

2.1. Deterministic analysis

Consider first the dynamics of the SIR epidemic model, representing the simplest compartmental approach to modelling infectious disease transmission of microparasites (Anderson and May, 1992), where $S(t)$, $I(t)$ and $R(t)$ represent the number of susceptible, infectious and recovered individuals at time t. If β represents the pathogen transmission rate and γ the recovery rate (such that $1/\gamma$ is the average duration of infectiousness), the model dynamics in a closed population (of size $N=S+I+R$) in the absence of demography are captured by the simple ODEs

$$\dot{S} = -\frac{\beta SI}{N},$$
$$\dot{I} = \frac{\beta SI}{N} - \gamma I \tag{1}$$

and subject to the initial conditions $S(0)=S_0$, $I(0)=I_0$ and $R(0)=0$. However, during the early stages of an outbreak when the number of infectious individuals is small, $S/N \approx 1$ and the number of infected individuals is given by

$$\dot{I} \approx \beta I - \gamma I, \tag{2}$$

which is readily solved as $I(t)=I_0 e^{(\beta-\gamma)t}$. We can equivalently rewrite this solution in terms of the basic reproduction number R_0, representing the average number of secondary individuals infected per primary case in an entirely susceptible population, and average generation time T_G, representing the average time from an individual becoming infected to themselves passing on infection to a secondary case, when transmission is independent of time as

$$I(t) = I_0 e^{((R_0-1)t)/T_G} \tag{3}$$

where $R_0=\beta/\gamma$ and $T_G=1/\gamma$, from which it is clear that the deterministic epidemic grows exponentially whenever $R_0>1$. The doubling time of the outbreak T_D, the duration of time for the initial number of cases to double, can be immediately derived as $T_D=T_G \ln 2/(R_0-1)$.

2.2. Stochastic analysis

The linearisation of (1) in the absence of saturation effects early on means that the number of infectious individuals in the SIR model corresponds to a simple birth–death process in a stochastic framework during the invasion stage, with per capita birth and death rates β and γ, respectively. If we define $p_i(t)$ as the probability that we have i infectious individuals at time t, the relevant master equation is

$$\frac{dp_i(t)}{dt} = -(\beta+\gamma)ip_i(t) + \gamma(i+1)p_{i+1}(t) + \beta(i-1)p_{i-1}(t). \tag{4}$$

Defining the probability generating function $G(z,t) = \sum_{i=0}^{\infty} p_i(t)z^i$ transforms (4) to the first-order PDE

$$\frac{\partial G(z,t)}{\partial t} = (z-1)(\beta z-\gamma)\frac{\partial G(z,t)}{\partial z}, \tag{5}$$

which may be solved using Lagrange's method of characteristics. Upon solution, the original probabilities may be obtained as

$p_i(t)=G^{(i)}(0,t)/i!$ where $G^{(i)}(z,t)$ refers to the ith derivative of $G(z,t)$ with respect to z. We consider two possible initial conditions.

Case I: Known initial conditions: For the case where $I(0)=I_0$ and hence $p_i(0)=\delta_{il_0}$ (where δ_{ij} is the Kronecker delta), we solve (5) subject to $G(z,0)=z^{I_0}$, leading to the solution

$$G(z,t)=\left(\frac{(z-1)+(1-R_0z)e^{-((R_0-1)t)/T_G}}{R_0(z-1)+(1-R_0z)e^{-((R_0-1)t)/T_G}}\right)^{I_0}. \quad (6)$$

The probability of extinction as the outbreak unfolds under Case I is given by substituting $z=0$ into (6) (Fig. 1(a)), giving $(1/R_0)^{I_0}$ as the asymptotic probability of extinction. It is clear, however, that this result overestimates the true likelihood of fade-out during the early stages of an outbreak, since the birth–death model only works as an approximation when the number of infectious individuals is a small fraction of the total population. A more reasonable estimate of the extinction probability may be obtained by evaluating (6) at a more appropriate outbreak time, namely the doubling time T_D, so that substituting $t=T_D=T_G\ln 2/(R_0-1)$ and $z=0$ into (6) gives the fade-out probability at this point as $(1/(2R_0-1))^{I_0}$. This is a factor of $(2-1/R_0)^{I_0}$ less than the asymptotic result, e.g. for an outbreak with $R_0=2$ seeded by one individual, $P_0(\infty)=1/2$, while $P_0(T_D)=1/3$ (Fig. 1(b)). It is clear from Fig. 1(b) that, in this case, the likelihood of fade-out is considerably more sensitive to the number of individuals seeding the outbreak than the basic reproduction number, highlighting the importance of contact tracing and local surveillance to rapidly identify potentially infected individuals, the role of asymptomatic infectious individuals in determining the effectiveness of early disease control (Fraser et al., 2004) and the difficulty in containing outbreaks with multiple infection foci, even for pathogens with a low reproduction number.

Case II: Uncertain initial conditions: For the case of uncertain initial conditions where the initial number of infectious individuals is Poisson distributed with mean I_0 and hence $p_i(0)=e^{-I_0}I_0^i/i!$, we solve (5) subject to $G(z,0)=e^{-I_0(z-1)}$, leading to the solution

$$G(z,t)=\exp\left(\frac{I_0(1-R_0)(1-z)}{R_0(1-z)-(1-R_0z)e^{-((R_0-1)t)/T_G}}\right). \quad (7)$$

It is readily shown by substituting $z=0$ that the asymptotic probability of fade-out under Case II is $\exp(I_0(1-R_0)/R_0)$, while estimation at the outbreak doubling time gives the extinction probability $\exp(2I_0(1-R_0)/(2R_0-1))$. For an $R_0=2$ outbreak seeded by drawing a random number of infectious individuals from a Poisson distribution with unit mean, $p_0(\infty)=e^{-1/2}\approx 0.61$ and $p_0(T_D)=e^{-2/3}\approx 0.51$, demonstrating the higher probability of fade-out in outbreaks with uncertainty in the initial conditions for a given R_0 (Fig. 2), and the difference becomes increasingly evident as R_0 increases. For outbreaks seeded with a mean of only one or two individuals, there is a significantly greater probability of fade-out in Case II compared to Case I and this does not become vanishingly small at large R_0 due to the non-zero proportion of

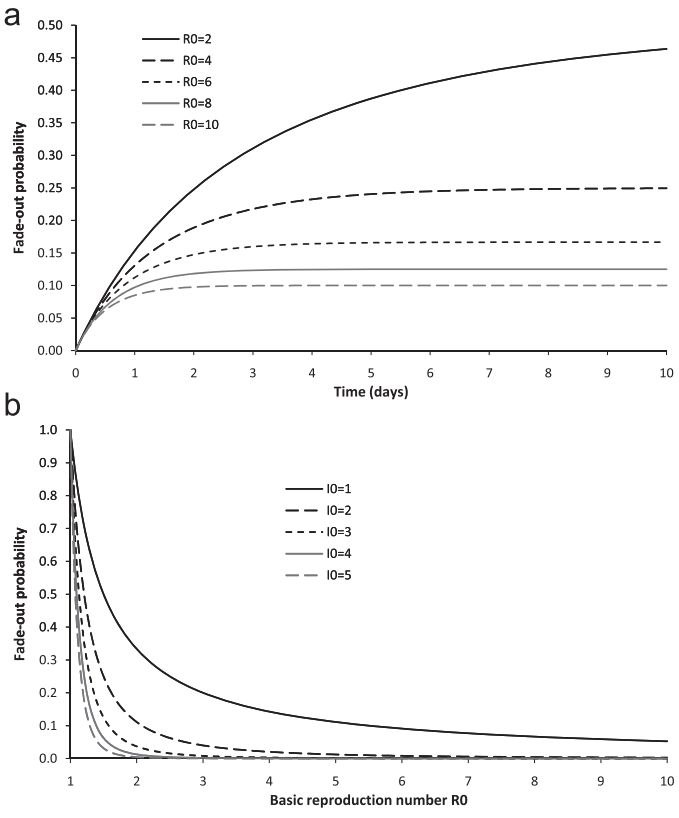

Fig. 1. For the unforced SIR model, (a) $p_0(t)$ for Case I with $I_0=1$ and $T_G=5$ days for different R_0 and (b) the instantaneous fade-out probability p_0 for Case I at the doubling time T_D as a function of R_0 and I_0.

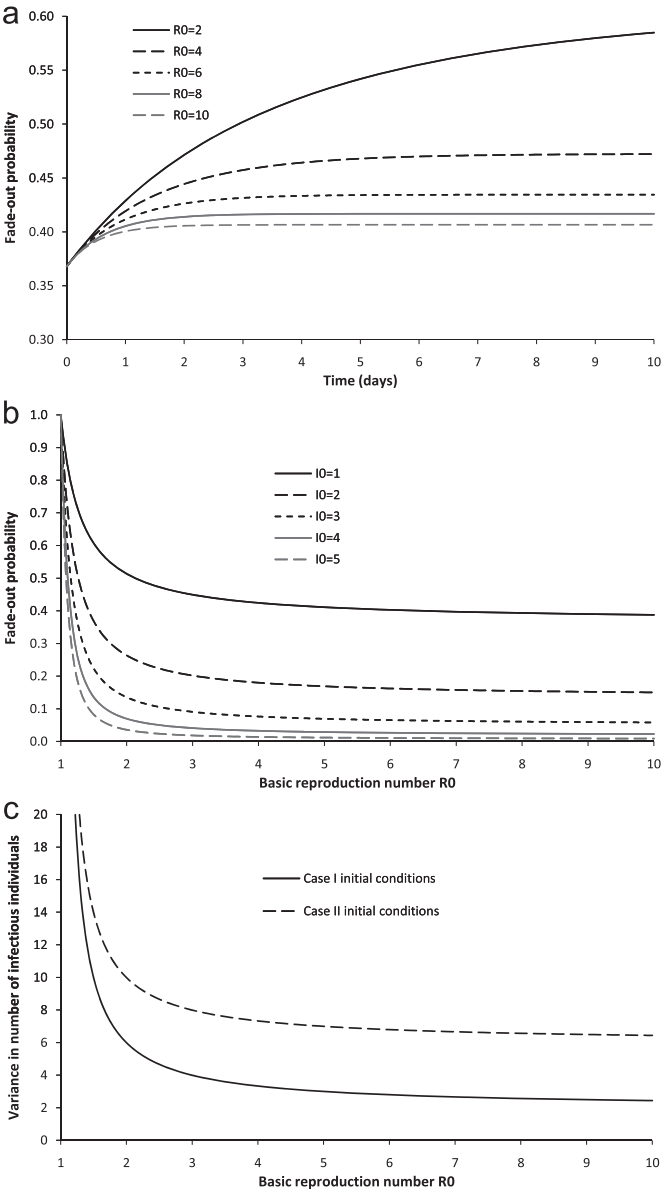

Fig. 2. For the unforced SIR model, (a) $p_0(t)$ for Case II with $I_0=1$ and $T_G=5$ days for different R_0, (b) the instantaneous fade-out probability p_0 for Case II at the doubling time T_D as a function of R_0 and I_0 and (c) $\mathrm{Var}(I(T_D))$ as a function of R_0 for Cases I and II initial conditions (illustrated for $I_0=1$).

outbreaks that do not take-off due to initial seeding with zero infectious individuals. It is also clear that independent of any uncertainty in the initial conditions, outbreak dynamics are more sensitive to the initial number of cases than the reproduction number of the pathogen, a result that has important implications for mitigation and control policies.

We can calculate the mean and variance of the number of infectious individuals from $E(I(t))=G'(1,t)$ and $\mathrm{Var}(I(t))=G'(1,t)+G'(1,t)-(G'(1,t))^2$, respectively. For Cases I and II, we obtain $E(I(t))=I_0e^{((R_0-1)t)/T_G}$, which, as expected, agrees with the deterministic solution, while the variance is given by

$$\mathrm{Var}(I(t))=\frac{I_0(R_0+1)}{(R_0-1)}e^{((R_0-1)t)/T_G}\left(e^{((R_0-1)t)/T_G}-1\right) \tag{8}$$

in Case I and

$$\mathrm{Var}(I(t))=I_0e^{((R_0-1)t)/T_G}\left(1-2R_0+2R_0e^{((R_0-1)t)/T_G}\right) \tag{9}$$

in Case II. Evaluating (8) and (9) at the doubling time T_D to illustrate the variability in these scenarios early on gives $\mathrm{Var}(I(T_D))=2I_0(R_0+1)/(R_0-1)$ and $\mathrm{Var}(I(T_D))=2I_0(3R_0-1)/(R_0-1)$ for Cases I and II, respectively, with variability in early case numbers directly proportional to the number of seeding individuals in both scenarios. Thus, there is considerably more variability in the case of uncertainty in the initial conditions by a factor of $(3R_0-1)/(R_0+1)$, tending to a factor of three as R_0 increases. This greater variability for a given R_0 (Fig. 2(c)) is consistent with the higher extinction probability under these conditions; for a given average number of cases, we must also have large outbreaks to compensate for those outbreaks that fade-out and thus the variance in the initial number of cases increases (see also Miller et al., 2010). It should be noted that this difference in variability is independent of I_0 and depends only on the reproduction number.

3. The forced SIR model

We now consider how the previous analysis and insights are modified for the SIR model in the presence of temporally forced transmission. Models which additionally have $\gamma=\gamma(t)$ will not be explicitly considered, since the linearity of the problem results in the analysis being readily extendable to this case. It should be noted, however, that such systems arise in climatically driven vector-borne disease models where vector survival is dependent on temperature and rainfall (Martens, 1998).

The functional form of the forcing term used to drive infectious disease models has been shown to profoundly affect the resultant disease dynamics (Keeling and Rohani, 2007). Here, we consider two functional forms, namely a simple sinusoid of the form

$$\beta(t)=\beta_0(1+\beta_1\cos\omega t) \tag{10}$$

and the two-state forcing term

$$\beta(t)=\beta_0(1\pm\beta_1), \tag{11}$$

where the plus and minus sign, respectively, correspond to high and low transmission seasons. In many applications, (11) is modified for systems that spend unequal durations of time with high and low transmission, with the most common example that of fewer days of low transmission between school children due to the structure of the school year in the case of measles, but the generalisation of the subsequent analysis to this case is straightforward and we only consider (11) to reduce the number of parameters and complexity of the analysis.

In both cases, β_0 represents the average transmission rate over one period and $\beta_0\beta_1$ the maximum amplitude of the variation in transmission about the mean, so that $\beta_0=0.1$ corresponds to a transmission rate 10% greater than the mean. While we consider only deterministically forced transmission models, it should be noted that the temporal forcing mechanisms of many systems are often subject to variability themselves. Thus, such systems are, in general, doubly stochastic with the form of the forcing function taking the form of (10) or (11) plus a noise term, but we do not pursue this here.

3.1. Deterministic analysis

For time-dependent disease transmission, integrating the equivalent form of (1) with $\beta=\beta(t)$, subject to I_0 initially infectious individuals, gives

$$I(t)=I_0e^{-\gamma t+\int_0^t\beta(t)dt}, \tag{12}$$

whereupon

$$I(t)=I_0e^{(\beta_0-\gamma)t}\underbrace{e^{((\beta_0\beta_1)/\omega)\sin\omega t}} \tag{13}$$

for forcing function (10). The underbrace denotes the modification factor to the constant transmission case due to temporal forcing and where the basic reproduction number continues to be given by $R_0=\beta_0/\gamma$. With sinusoidal forcing, the impact of periodicity in $\beta(t)$ is determined by ω, since for periodic changes in transmission that occur on short timescales compared to outbreak dynamics (characterised by the generation time T_G), the baseline outbreak behaviour is strongly modulated by the shape of the sinusoidal forcing. However, for annual forcing (where ω_t is relatively small), the impact of oscillatory behaviour on outbreak timescales is likely to be minimal.

For the forcing function (11), if the timescale of seasonal changes in transmission is long compared to the timescale of the outbreak dynamics, the resultant difference in prevalence $\Delta I(t)$ between the higher and lower transmission regimes is given by

$$\Delta I(t)=I_0e^{(\beta_0-\gamma)t}\underbrace{2\sinh\beta_0\beta_1t}, \tag{14}$$

where the underbrace again denotes the effect on the invasion dynamics of differences in transmission from the baseline case of constant transmission β_0. In this case, $R_0=\beta_0/\gamma$ only if the durations of the high and low transmission regimes are equal in length. In addition, if we have rapid initial growth of the epidemic and the timescale of changes in transmission is short compared to the timescale of the outbreak dynamics, it is worth noting that the assumption of linearity in the transmission model may break down before the transition from high to low transmission in (11) can occur. Either way, it is clear from (13) and (14) that small changes in transmission have a strong effect on increasing prevalence compared to the case of constant transmission and this increases exponentially with the amplitude of forcing β_1, e.g. a 49% and 82% increase in prevalence at $t=2T_G$ and $t=3T_G$, respectively, for a 10% increase in transmission (Fig. 3). This exponential effect becomes stronger still with increasing R_0, while the initial conditions have only a linear effect on prevalence.

3.2. Stochastic analysis

The equivalent stochastic system for the forced SIR model is the non-homogeneous birth–death process, with the relevant PDE for $G(z,t)$ given by substituting $\beta=\beta(t)$ into (5). If we define

$$J(t)=\int_0^t\beta(\tau)e^{\gamma\tau-\int_0^\tau\beta(\tau')d\tau'}d\tau, \tag{15}$$

solution via the method of characteristics gives

$$G(z,t)=\left(\frac{(z-1)+e^{\gamma t-\int_0^t\beta(\tau)d\tau}-(z-1)J(t)}{e^{\gamma t-\int_0^t\beta(\tau)d\tau}-(z-1)J(t)}\right)^{I_0} \tag{16}$$

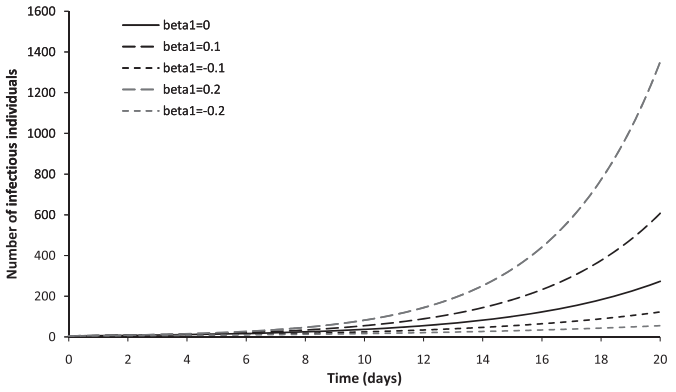

Fig. 3. $I(t)$ for the SIR model with constant transmission ($\beta_1=0$) and the forcing function (11) with 10% ($\beta_1=\pm 0.1$) and 20% ($\beta_1=\pm 0.2$) changes in transmission (where $T_G=5$ days, $I_0=5$ and $R_0=2$).

Table 1
Extinction probability and variance of the forced SIR model under Cases I and II initial conditions (where $\rho(t)=\gamma t-\int_0^t \beta(\tau)\mathrm{d}\tau$).

	Case I	Case II
$p_0(t)$	$\left(\frac{e^{\rho(t)}+J(t)-1}{e^{\rho(t)}+J(t)}\right)^{I_0}$	$\exp\left(\frac{-I_0}{e^{\rho(t)}+J(t)}\right)$
$\mathrm{Var}(I(t))$	$I_0e^{-2\rho(t)}(2J(t)+e^{\rho(t)}-1)$	$I_0e^{-\rho(t)}(1+2J(t)e^{-\rho(t)})$

for Case I and

$$G(z,t)=\exp\left(\frac{I_0(z-1)}{e^{\gamma t-\int_0^t \beta(\tau)\,d\tau}-(z-1)J(t)}\right) \tag{17}$$

for Case II. In both cases, the mean is given by

$$E(I(t))=I_0e^{-\gamma t+\int_0^t \beta(\tau)d\tau}, \tag{18}$$

which agrees with the deterministic solution. The extinction probability and variance in each case is shown in Table 1. It is clear, however, that the analytical tractability of the forced SIR model is strongly dependent on the functional form of the transmission function. Indeed, computation of $J(t)$ for (10) and most realistic functions with an explicit time-dependence is not possible and although integral approximations may be developed, we solely consider (11) as our function. It is also worth noting that $J(t)$, and hence $p_0(t)$, may be analytically calculated only in the case of constant transmission or where $\beta(t)$ depends linearly on time; any non-linear transmission function, periodic or otherwise, prevents exact calculation (although may, of course, be calculated numerically). However, it is readily seen, given the form of the integrand in (15), that the extinction probability depends considerably more strongly on early transmission rates than those later on, with this dependence decaying approximately exponentially with time. We note also that further theoretical and numerical analysis contrasting the effects of the functional form of $\beta(t)$ (and doubly stochastic functions) on outbreak dynamics is postponed to future work.

Seasonal increases in transmission lead to smaller likelihoods of extinction following an outbreak (Fig. 4a), with the probability increasing with additional uncertainty in initial conditions, partially due to the fact that $p_0(0)=0$ for Case I, while $p_0(0)=e^{-I_0}$ for Case II. The linear nature of the system and form of the forcing function means that linear changes in β_1 lead to approximately linear changes in $p_0(t)$. As in the unforced system, the biggest contribution to early fade-out is from the initial conditions (and any uncertainty therein), with the role of R_0 and seasonality (for most realistic values of β_1) assuming a far less

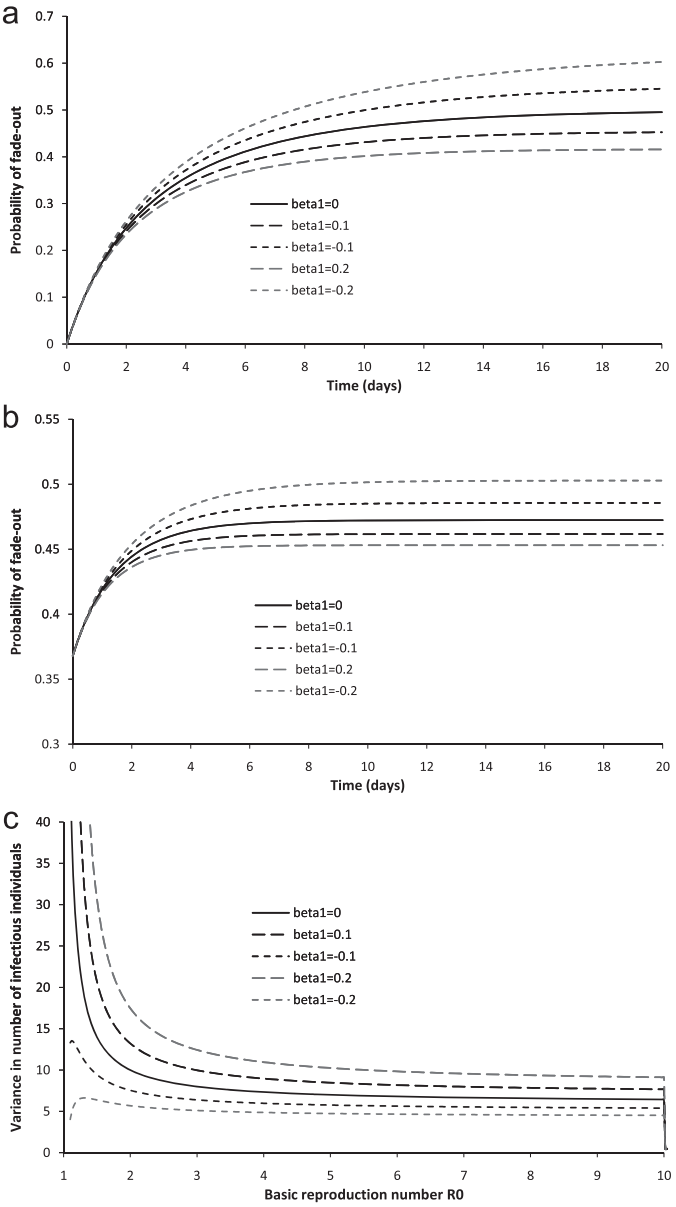

Fig. 4. $p_0(t)$ at different β_1 for (a) Case I with $R_0=2$ and (b) Case II with $R_0=4$. (c) $\mathrm{Var}(I(T_{D0}))$ as a function of R_0 for different values of β_1 for Case II (where T_{D0} is the doubling time of the associated unforced system). In all cases, $T_G=5$ days and $I_0=1$.

important role, although it should be noted that this may vary with other functional forms with larger amplitude changes in $\beta(t)$ over short timescales. As R_0 increases, $p_0(t)$ reduces and tends to its equilibrium value more rapidly and increasing seasonality has less effect on fade-out as R_0 increases. At low R_0, small perturbations in transmission can take the system below $R_0=1$, while considerably larger perturbations are required to have a comparable effect at larger R_0 (Fig. 4b).

Increasing β_1 also increases the variance in the number of cases for a given R_0, particularly at lower R_0. By comparing to the $\beta_1=0$ case, we can better understand the contrasting roles of stochasticity and seasonality. At small β_1, the linearity of the system means that stochasticity in the underlying disease processes plays a more significant role when R_0 is large, while at small R_0, the majority of the variance may be attributed to seasonal changes in transmission (e.g. a 10% increase in transmission in Case I accounts for 72% of the variance when $R_0=1.1$, but only 17% of the variability when $R_0=6$). However, the role of seasonality clearly increases with β_1 and only

moderate levels of seasonality are required to dominate the variability arising from disease processes, even at large R_0. Finally, note that the role of seasonality versus stochasticity is relatively independent of any uncertainty in the initial conditions when β_1 is small, with the role in Cases I and II very similar despite the additional source of variability from the initial conditions in the latter, while there is considerably greater sensitivity to β_1 in the full non-linear system.

4. The unforced SEIR model

4.1. Deterministic analysis

We now consider the SEIR epidemic model, where the additional compartment tracks the number of individuals who are infected, but not yet infectious, with the pathogen at time t and we denote this by $E(t)$. If σ represents the rate at which individuals become infectious (so that $1/\sigma$ represents the average duration of latency), the model dynamics in a closed population (of size $N=S+E+I+R$) in the absence of demography are given by

$$\begin{aligned}\dot{S} &= -\frac{\beta SI}{N},\\ \dot{E} &= \frac{\beta SI}{N}-\sigma E,\\ \dot{I} &= \sigma E-\gamma I,\end{aligned} \tag{19}$$

with the additional initial condition $E(0)=E_0$. Under the invasion approximation $S/N\approx 1$, the system reduces to

$$\begin{pmatrix}\dot{E}\\ \dot{I}\end{pmatrix}=\begin{pmatrix}-\sigma & \beta\\ \sigma & -\gamma\end{pmatrix}\begin{pmatrix}E\\ I\end{pmatrix}, \tag{20}$$

whereupon calculating the eigenvalues r of the matrix $M=\begin{pmatrix}-\sigma & \beta\\ \sigma & -\gamma\end{pmatrix}$ requires solution of the characteristic equation

$$r^2+(\sigma+\gamma)r+\sigma(\gamma-\beta)=0, \tag{21}$$

so that since $R_0=\beta/\gamma$, we obtain

$$r=\frac{1}{2}\left(-(\sigma+\gamma)\pm\sqrt{(\sigma+\gamma)^2+4\sigma\gamma(R_0-1)}\right), \tag{22}$$

from which it is again clear that the epidemic requires $R_0>1$ to take-off. Denoting the two solutions as r_1 and r_2 for the positive and negative roots, respectively, we obtain

$$I(t)=Ae^{r_1 t}+Be^{r_2 t}, \tag{23}$$

whereupon imposing the initial conditions $E(0)=E_0$ and $I(0)=I_0$ gives $A=(\sigma E_0-I_0(\gamma+r_2))/(r_1-r_2)$ and $B=(\sigma E_0-I_0(\gamma+r_1))/(r_2-r_1)$. When $R_0>1$, $r_1>1$ and $r_2>0$ always and the first term in (23) dominates, with the ratio $I(t)/E(t)$ tending towards the equilibrium distribution $(I/E)^*=(r_2+\sigma)/\beta$, found by calculating the eigenvector corresponding to the eigenvalue r_1. Note that if the system does not initially possess the equilibrium distribution, the difference between the system with $E(0)=E_0$ and $I(0)=I_0$ and $(I/E)^*$ in the direction of the (smaller) eigenvector of M (corresponding to r_2) decays over time at rate r_2.

Thus, while we cannot uniquely define the real-time growth rate in this model, it is clear that as the outbreak progresses (but before the depletion of susceptibles takes effect), the first term on the RHS of (23) increasingly dominates such that the doubling time T_D is approximately given by $\ln 2/r_1$. The average generation time in this model is $T_G=1/\sigma+1/\gamma$, but unlike the SIR model, we are unable to reparameterise the growth rate only in terms of R_0 and T_G.

4.2. Stochastic analysis

In the stochastic representation of the SEIR model, exposed individuals give rise to infectious individuals when they die at per capita rate σ, while infectious individuals give birth to exposed individuals at per capita rate β and die at rate γ. If we let $p_{ij}(t)$ represent the probability that we have i exposed and j infectious individuals at time t, the master equation becomes

$$\begin{aligned}\frac{dp_{ij}(t)}{dt} &= -((\beta+\gamma)j+\sigma i)p_{ij}(t)+\beta j p_{i-1j}(t)\\ &\quad+\sigma(i+1)p_{i+1j-1}(t)+\gamma(j+1)p_{ij+1}(t).\end{aligned} \tag{24}$$

By extension to the method of solution in Section 2.2, we define the joint probability generating function $G(z_1,z_2,t)=\sum_{i,j=0}^{\infty}p_{ij}(t)z_1^i z_2^j$, multiply (24) by $z_1^i z_2^j$ and sum each term over i and j to obtain

$$\begin{aligned}\frac{\partial G(z_1,z_2,t)}{\partial t} &= \sigma(z_2-z_1)\frac{\partial G(z_1,z_2,t)}{\partial z_1}+(\gamma(1-z_2)\\ &\quad+\beta z_2(z_1-1))\frac{\partial G(z_1,z_2,t)}{\partial z_2}.\end{aligned} \tag{25}$$

Solution of (25) via Lagrange's method, however, can only be written in terms of a characteristic ODE that, to the best of our knowledge, cannot be solved exactly. Although this means that an exact expression for the fade-out probability of the SEIR model cannot be derived, we can calculate moments of the underlying probability distribution.

Let us first define the joint moment generating function $M(\theta_1,\theta_2,t)=\sum_{i,j=0}^{\infty}p_{ij}(t)e^{\theta_1 i}e^{\theta_2 j}$, so that comparing to the definition of $G(z_1,z_2,t)$ and making the substitutions $z_k=e^{\theta_k}$ and $\partial z_k=e^{\theta_k}\partial\theta_k$ for $k=1$, 2 maps (25) onto a PDE in $M(\theta_1,\theta_2,t)$, which, upon expansion, allows calculation of the marginal and joint moments about zero. Since we are particularly interested in the variance early on, we switch to cumulants, rather than moments. Defining the cumulant generating function $K(\theta_1,\theta_2,t)=\sum_{i,j=0}^{\infty}K_{ij}(t)(\theta_1^i/i!)(\theta_2^j/j!)$ (where k_{ij} are the joint cumulants) and making the substitutions $K(\theta_1,\theta_2,t)=\ln M(\theta_1,\theta_2,t)$ and $\partial M(\theta_1,\theta_2,t)=e^k\partial K(\theta_1,\theta_2,t)$ gives

$$\frac{\partial K(\theta_1,\theta_2,t)}{\partial t}=\sigma(e^{\theta_2-\theta_1}-1)\frac{\partial K(\theta_1,\theta_2,t)}{\partial\theta_1}+\left(\gamma e^{-\theta_2}+\beta e^{\theta_1}-\gamma-\beta\right)\frac{\partial K\theta_1,\theta_2,t)}{\partial\theta_2}. \tag{26}$$

Substituting the definition of $K(\theta_1,\theta_2,t)$ into (26), expanding the exponentials as a power series and equating coefficients of θ_1 and θ_2 gives the first cumulant equations

$$\begin{aligned}\kappa'_{10} &= \beta\kappa_{01}-\sigma\kappa_{10},\\ \kappa'_{01} &= \sigma\kappa_{10}-\gamma\kappa_{01},\end{aligned} \tag{27}$$

while expanding for the covariances by equating coefficients of θ_1^2, θ_2^2, and $\theta_1\theta_2$ gives

$$\begin{aligned}\kappa'_{20} &= 2\beta\kappa_{11}+\beta\kappa_{01}-2\sigma\kappa_{20}+\sigma\kappa_{10},\\ \kappa'_{02} &= -2\gamma\kappa_{02}+\gamma\kappa_{01}+2\sigma\kappa_{11}+\sigma\kappa_{10},\\ \kappa'_{11} &= \beta\kappa_{02}-\gamma\kappa_{11}-\sigma\kappa_{11}+\sigma\kappa_{20}-\sigma\kappa_{10}.\end{aligned} \tag{28}$$

We consider again two initial conditions.

Case I: Known initial conditions: For the case where $E(0)=E_0$, $I(0)=I_0$ and hence $p_{ij}(0)=\delta_{iE_0}\delta_{jI_0}$, we have $G(z_1,z_2,0)=z_1^{E_0}z_2^{I_0}$, $M(\theta_1,\theta_2,0)=e^{\theta_1 E_0}e^{\theta_2 I_0}$ and thus $K(\theta_1,\theta_2,0)=\theta_1 E_0+\theta_2 I_0$. This immediately implies that $k_{10}(0)=E_0$, $k_{01}(0)=I_0$ and $k_{ij}(0)=0$ for all other ij combinations.

Case II: Uncertain initial conditions: For the case of uncertain initial conditions where $E(0)\sim P0(E_0)$, $I(0)\sim P0(I_0)$ and hence $p_{ij}(0)=(e^{-E_0}E_0^i/i!)(e^{-I_0}I_0^j/j!)$, we have $G(z_1,z_2,0)=e^{E_0(z_1-1)}e^{I_0(z_2-1)}$,

$M(\theta_1,\theta_2,0)=\exp(E_0(e^{\theta_1}-1)+I_0(e^{\theta_2}-1))$ and thus $K(\theta_1,\theta_2,0)=\ln M(\theta_1,\theta_2,0)=(E_0(e^{\theta_1}-1)+I_0(e^{\theta_2}-1))$. Expanding the RHS in terms of cumulants and evaluating at $t=0$ implies that $\kappa_{i0}(0)=E_0$ for all i, $\kappa_{0j}(0)=I_0$ for all j and $\kappa_{ij}(0)=0$ for all other ij combinations.

It is readily shown, through similar analysis to Section 4.1, that

$$\kappa''_{01}+(\sigma+\gamma)\kappa'_{01}+\sigma(\gamma-\beta)\kappa_{01}=0, \tag{29}$$

with solution

$$\kappa_{01}(t)=Ae^{r_1t}+Be^{r_2t}, \tag{30}$$

where A, B, r_1 and r_2 are identical to the definitions in Section 4.1, while

$$\kappa_{10}(t)=Ce^{r_1t}+De^{r_2t} \tag{31}$$

where $C=(\beta I_0-\sigma E_0-E_0r_2)/(r_1-r_2)$ and $D=(\beta I_0-\sigma E_0-E_0r_1)/(r_2-r_1)$. Both results agree, as expected, with the deterministic solution. Similar manipulation of the second-order cumulant equations leads to non-homogeneous equations with constant coefficients of the form

$$A_3\kappa'''_{02}+A_2\kappa''_{02}+A_1\kappa'_{02}+A_0\kappa_{02}=f(t), \tag{32}$$

where A_k (for $k=0, 1, 2, 3$) are constants dependent on β, σ and γ and $f(t)$ arises from the dependence of the covariances on the means $k_{01}(t)$ and $k_{10}(t)$. While exactly solvable, (32) gives solutions for Cases I and II that are too unwieldy to reproduce or provide significant insight and we thus proceed numerically. Note that both k_{20} and k_{11} follow identical equations structurally to (32), but with different definitions of A_k.

As with the stochastic SIR model, we consider the variability in prevalence as a function of R_0 at the doubling time T_D, calculated as the solution of

$$2I_0=Ae^{r_1T_D}+Be^{r_2T_D}, \tag{33}$$

from which it is clear that, unlike the SIR model, a closed form expression for T_D in terms of R_0 and T_G is not possible. However, numerical solution of (33) is straightforward and Fig. 5 contrasts the variability of the SIR and SEIR models for Cases I and II initial conditions. As expected, there is greater variability in prevalence under Case II compared to Case I and this difference increases with R_0. For a given set of initial conditions and R_0, the variability in prevalence is always greater in the SEIR model, particularly when R_0 is small, due to the additional process of latency. As R_0 increases, however, the two models converge in variability and this holds independent of whether we impose Case I or Case II conditions. It is also worth noting that when $R_0<1.5$, inclusion of the latency process may generate greater variability in prevalence than the equivalent SIR model with uncertain initial conditions when I_0 is small (Fig. 5).

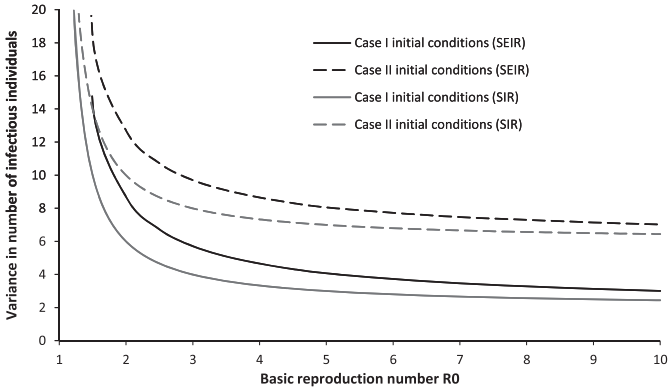

Fig. 5. $k_{02}(T_D)=\mathrm{Var}(I(T_D))$ as a function of R_0 for Cases I and II initial conditions for the unforced SEIR model (where $E_0=0$, $I_0=1$ and the average latent and infectious periods are 2 and 3 days, respectively).

5. The forced SEIR model

5.1. Deterministic analysis

As with the forced SIR model, analytical tractability of the system reduces considerably in the presence of explicit temporally forced transmission, but progress can be made in the deterministic case. For the general case $\beta=\beta(t)$, the number of infectious individuals is given by the solution to

$$\ddot{I}+(\sigma+\gamma)\dot{I}+\sigma(\gamma-\beta(t))I=0 \tag{34}$$

and the nature of the solution is strongly dependent on the form of $\beta(t)$. For the simple two-state forcing function (11), substituting $I(t)=e^{rt}$ gives

$$r=\frac{1}{2}\left(-(\sigma+\gamma)\pm\sqrt{(\sigma+\gamma)^2+4\sigma(\beta_0(1\pm\beta_1)-\gamma)}\right), \tag{35}$$

so that

$$I(t)=Ae^{r_3t}+Be^{r_4t} \tag{36}$$

where r_3 and r_4 are the positive and negative roots of (35), respectively, and A and B are identical to the definitions in Section 4.1. For the sinusoidal forcing function (10), substituting into (34) gives the solution

$$I(t)=e^{-(1/2)(\gamma+\sigma)t}\left(\alpha_1C\left(a,q,\frac{1}{2}\omega t\right)+\alpha_2S\left(a,q,\frac{1}{2}\omega t\right)\right) \tag{37}$$

where $C(a,q,\frac{1}{2}\omega t)$ and $S(a,q,\frac{1}{2}\omega t)$ are the even and odd Mathieu functions, respectively, with characteristic value $a=(2\gamma\sigma-\gamma^2-4\beta_0\sigma-\sigma^2)/\omega^2$ and parameter $q=2\beta_0\beta_1\sigma/\omega^2$. Substituting the initial conditions and using the fact that $C(a, q, 0)=S'(a, q, 0)=1$ and $C'(a, q, 0)=S(a, q, 0)=0$ gives $\alpha_1=I_0$ and $\alpha_2=1/2(\sigma(2E_0+I_0)-\gamma I_0)$.

Unlike the SIR model, the prevalence cannot be written as a product of a constant transmission term and modulation factor arising from seasonal forcing, so we resort to numerical analysis of (36) (Fig. 6(a)). As with the forced SIR model, small changes in β_1 can have strong non-linear influences on increasing prevalence compared to the case of constant transmission, e.g. a 31% and 51% increase in prevalence at $t=2T_G$ and $t=3T_G$, respectively, for a 10% increase in transmission (cf. Section 3.1), particularly true with increasing R_0, although small changes in transmission take longer to propagate through the system and affect prevalence due to the delay of latency. The addition of latency into the model slows the rate at which prevalence increases, so that at any given time and R_0, the mean prevalence will be lower in the SEIR model than the SIR model. Thus, the effect of temporal forcing is reduced since there is more underlying stochasticity in the system and this dominates the dynamics when β_1 is relatively small. Although intractable to demonstrate analytically for the SEIR model, the effect of increasing β_1 on prevalence is also exponential, while the initial conditions additionally play a stronger role.

5.2. Stochastic analysis

As with the equivalent model incorporating temporally forced transmission in the stochastic SIR framework, analytical progress with an explicit time-dependence in $\beta(t)$ is limited to reduction of the problem to a characteristic ODE that cannot be solved exactly. However, as with the SIR model, progress can be made for the 2-state forcing function. Substituting (11) into (27) and (28) gives solutions for the means that agree with the deterministic analysis, while solving for the second-order cumulants gives equations of the form

$$A_3(t)\kappa'''_{02}+A_2(t)\kappa''_{02}+A_1(t)\kappa'_{02}+A_0(t)\kappa_{02}=f(t) \tag{38}$$

for the variance of both Es and Is (where A_k for $k=0, 1, 2, 3$ are defined as per (32)). Once again, although (38) may, in principle, be solved exactly,

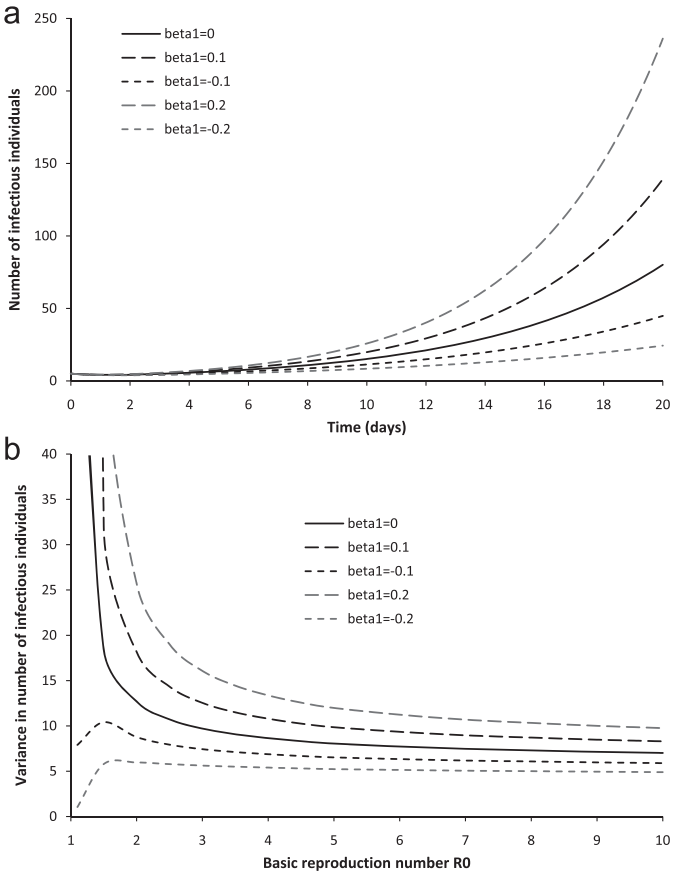

Fig. 6. (a) $k_{01}(t)=E(I(t))$ for the SEIR model with constant transmission and the forcing function (11) with 10% and 20% changes in transmission (where $E_0=0$, $I_0=5$, $R_0=2$ and we assume latent and infectious periods of 2 and 3 days, respectively). (b) $k_{02}(T_{D0})=\mathrm{Var}(I(T_{D0}))$ as a function of R_0 for different values of β_1 for Case II initial conditions for the forced SEIR model with forcing function (11) (where $E_0=0$, $I_0=1$ and we assume latent infectious periods of 2 and 3 days, respectively).

the solution is too complex to reproduce, so we instead equivalently substitute (11) into (28) and solve numerically to contrast the effect of temporal forcing in a stochastic setting with the case of constant transmission.

As in the SIR model, we find increasing variability in prevalence at the doubling time for fixed R_0 as the amplitude of short-term seasonality increases. There exists greater variability in the SEIR model (compared to the SIR model) due to the additional stochastic process of latency, although the two models converge as R_0 increases since transmission increasingly dominates this delay. Contrasting the roles of stochasticity and seasonality, we find that seasonality predominantly dominates when R_0 is small (and close to unity), e.g. a 10% increase in transmission in Case II accounts for 88% of the variance when $R_0=1.1$, but only 17% of the variability when $R_0=6$, while stochasticity dominates as R_0 increases. The threshold value of R_0 where seasonality and stochasticity equally contribute to the variance is approximately 1.2 for the SIR model and 1.4 for the SEIR model for the parameters in Fig. 6 when $\beta_1=0.1$, so that for infectious diseases with a delay between infection and infectiousness and $R_0>1.4$, this highlights the importance of stochasticity in driving outbreak dynamics when the seasonal component is not too large.

Fig. 6 illustrates the strong non-linear dependence of the variability on β_1 and this holds for the SIR and SEIR models, although larger amplitude changes on outbreak timescales will affect this. The functional form of $\beta(t)$, plus any additional temporal variability in other disease processes, may also play a key role. Finally, we find that these results hold almost entirely independently of any additional uncertainty in the initial conditions when β_1 is small and this appears to be a standard result independent of the dimensionality of the system, although further analysis is required to verify this.

6. Conclusions

Although the power of master equations for simulating and deriving analytical insight into the behaviour of stochastic epidemic models has been recognised previously (Chen and Bokka, 2005; Grabowski and Kosinski, 2004; Keeling and Ross, 2008; Rozhnova and Nunes, 2009), we illustrate here how insight into the effects of temporal variability in transmission on stochastic infectious disease dynamics may also be incorporated within this framework. This is a key advance in the study of infectious disease dynamics, as much of the insight to date on the effects of seasonality on disease dynamics has resulted largely from analytical or numerical analysis of deterministic epidemic (or endemic) models (Bailey, 1975; Bolker and Grenfell, 1993; Dietz, 1976; Moneim, 2007; Stone et al., 2007). While the approach is applied to linearised epidemic models, we demonstrate here that this approach remains robust (and indeed linear in terms of probabilities) even for full non-linear disease systems, particularly when the aim is to gain a better understanding of the invasion dynamics of epidemic infections into vulnerable populations.

The first important outcome highlighted in this work is that while exact results regarding the role of stochasticity and seasonality early on in the presence of a temporally explicit forcing function are possible only for the SI epidemic model, the consideration of a 2-state forcing function (11) can lead to useful insights into more realistic disease models. In particular, we demonstrate in this regard that the master equation approach will allow useful insights into key epidemiological properties such as fade-out, emergence and initial spread rate, and variability in these variables, that would otherwise be less transparent, accessible and quantifiable simply through direct numerical simulation.

The application of this general framework to unforced SIR and SEIR models has illustrated the greater sensitivity of the early dynamics of these systems to the initial conditions rather than the basic reproduction number, particularly if there is additional uncertainty in the initial conditions. In particular, we show how stochasticity during the early stages of an outbreak when R_0 is close to unity will have a major effect on the probabilities of fade-out and establishment, as well as variability in prevalence in these systems, with the variability in prevalence greater for SIR models. By contrast, in forced models, the results show that while outbreak dynamics (fade outs, emergence and spread) are extremely sensitive to the amplitude of temporal forcing when R_0 is close to unity, stochastic effects quickly play a far stronger role than temporal variability as R_0 increases (almost independent of any additional uncertainty in the initial conditions). Small changes in transmission may, however, have exponential effects on prevalence early on, although the precise sensitivity is correlated with the dimensionality of the system and hence the amount of stochasticity arising from underlying disease processes. A key finding is that, in general, the effect of temporal forcing will be lower in the SEIR than the corresponding SIR model due to the additional process of latency.

These findings regarding the epidemiological properties of SIR and SEIR models during the invasion stage have thus not only produced new insights regarding forces that may govern the invasion probability of microparasitic diseases, but also raise interesting theoretical and applied questions that may be considered in future research. These include considering when

non-linear effects become important, since our analysis only considers the case where the depletion of susceptibles is not significant and we expect small amplitude changes in transmission to be amplified further by the non-linearities of full infectious disease models. As well as obtaining a better understanding of the effect of different forcing functions on outbreak dynamics, we also need to better understand the effects of forcing functions which themselves change over time, resulting in doubly stochastic models. Temporal variability in multiple disease processes also represent important challenges. The generic techniques and insights gained here may also be applied to many problems, and one example is improving our understanding of how changes in environmental conditions will affect the emergence of climatically driven infectious diseases, particularly vector-borne diseases, in geographic regions currently disease-free.

Overall, we have thus illustrated a valuable modelling framework for better understanding stochastic disease transmission under fluctuating, variable or uncertain drivers, which arguably represents the most realistic and general framework for assessing the impact of environmental changes on infectious disease transmission. We believe that such an approach may in particular represent the most realistic mechanistic modelling framework for investigating the potential and probable invasion of vector-borne microparasitic diseases, such as malaria and dengue, into susceptible populations as future climatic conditions become favourable for the transmission of these diseases in new areas (Parham and Michael, 2010). Present climate-driven transmission models for these diseases do not explicitly take account of the impact of the factors investigated here. Our results indicate that improving understanding of the impact of climate change on disease invasion dynamics will require a more realistic analysis of these factors, especially as increasing variability in climatic components has been linked to changes in malaria infection dynamics (McKenzie et al., 2001; Zhou et al., 2004).

Acknowledgements

The authors would like to thank two anonymous reviewers for comments that greatly improved this manuscript and the Grantham Institute for Climate Change at Imperial College London for support and funding of this research. EM acknowledges NIH Grant no. RO1 AI069387-01A1 for part support of this work.

References

Alonso, D., McKane, A., 2002. Extinction dynamics in mainland–island metapopulations: an *N*-patch stochastic model. Bulletin of Mathematical Biology 64, 913–958.

Altizer, S., et al., 2006. Seasonality and the dynamics of infectious diseases. Ecology Letters 9, 467–484.

Anderson, R.M., May, R.M., 1992. Infectious Diseases of Humans: Dynamics and Control. Oxford University Press.

Bacaër, N., 2007. Approximation of the basic reproduction number R_0 for vector-borne diseases with a periodic vector population. Bulletin of Mathematical Biology 69, 1067–1091.

Bacaër, N., Ouifki, R., 2007. Growth rate and basic reproduction number for population models with a simple periodic factor. Mathematical Biosciences 210, 647–658.

Bailey, N.T.J., 1975. The Mathematical Theory of Infectious Diseases and its Applications. Charles Griffin and Company, London.

Bolker, B.M., Grenfell, B.T., 1993. Chaos and biological complexity in measles dynamics. Proceedings of the Royal Society of London B 251, 75–81.

Chen, W.Y., Bokka, S., 2005. Stochastic modeling of nonlinear epidemiology. Journal of Theoretical Biology 234 (4), 455–470.

Conlan, A.J.K., Grenfell, B.T., 2007. Seasonality and the persistence and invasion of measles. Proceedings of the Royal Society of London B 274 (1614), 1133–1141.

Craig, M.H., et al., 1999. A climate-based distribution model of malaria transmission in Sub-Saharan Africa. Parasitology Today 15 (3), 105–111.

Dieckmann, U., Law, R., 1996. The dynamical theorey of coevolution: a derivation from stochastic ecological processes. Journal of Mathematical Biology 34, 579–612.

Dietz, K., 1976. The incidence of infectious diseases under the influence of seasonal fluctuations. Lecture Notes in Biomathematics 11, 1–15.

Duerr, H.P., Eichner, M., 2010. Epidemiology and control of onchocerciasis: the threshold biting rate of savannah onchocerciasis in Africa. International Journal for Parasitology 40 (6), 641–650.

Fraser, C., et al., 2004. Factors that make an infectious disease outbreak controllable. Proceedings of the National Academy of Sciences 101 (16), 6146–6151.

Grabowski, A., Kosinski, R.A., 2004. Epidemic spreading in a hierarchical social network. Physical Review E, 70. doi:10.1103/PhysRevE.70.031908.

Grassly, N.C., Fraser, C., 2006. Seasonal infectious disease epidemiology. Proceedings of the Royal Society B 273, 2541–2550.

Keeling, M., Rohani, P., 2007. Modeling Infectious Diseases in Humans and Animals. Princeton University Press.

Keeling, M.J., Grenfell, B.T., 2002. Understanding the persistence of measles: reconciling theory, simulation and observation. Proceedings of the Royal Society of London B 269, 335–343.

Keeling, M.J., Ross, J.V., 2008. On methods for studying stochastic disease dynamics. Journal of the Royal Society Interface 5, 171–181.

Kermack, W.O., McKendrick, A.G., 1927. A contribution to the mathematical theory of epidemics. Proceedings of the Royal Society of London A 115, 700–721.

Martens, P., 1998. Health and Climate Change: Modelling the Impacts of Global Warming and Ozone Depletion. Earthscan Publications Ltd., London.

Miller, J.C., et al., 2010. Epidemics with general generation interval distributions. Journal of Theoretical Biology 262 (1), 107–115.

McKenzie, F.E., et al., 2001. Seasonality, parasite diversity and local extinctions in *Plasmodium falciparum* malaria. Ecology 82 (10), 2673–2681.

Moneim, I.A., 2007. Seasonally varying epidemics with and without latent period: a comparative simulation study. Mathematical Medicine and Biology 24 (1), 1–15.

Parham, P.E., Michael, E., 2010. Modeling the effects of weather and climate change on malaria transmission. Environmental Health Perspectives 118 (5), 620–626.

Rozhnova, G., Nunes, A., 2009. Cluster approximations for infection dynamics on random networks. Physical Review E 80 (5). doi:10.1103/PhysRevE.80.051915.

Ruiz, D., et al., 2008. A multimodel framework in support of malaria surveillance and control. In: Thomson, M.C. (Ed.), Seasonal Forecasts, Climatic Change and Human Health. Springer Science and Business Media B.V., New York, pp. 101–125.

Stone, L., et al., 2007. Seasonal dynamics of recurrent epidemics. Nature 446, 533–536.

Stollenwerk, N., Briggs, K.M., 2000. Master equation solution of a plant disease model. Physics Letters A 274, 84–91.

Stollenwerk, N., Jansen, V.A.A., 2003. Meningitis, pathogenicity near criticality: the epidemiology of meningococcal disease as a model for acccidental pathogens. Journal of Theoretical Biology 222, 347–359.

Viet, A., Medley, G.F., 2006. Stochastic dynamics of immunity in small populations: a general framework. Mathematical Biosciences 200, 28–43.

Zhou, G., et al., 2004. Association between climate variability and malaria epidemics in the East African highlands. Proceedings of the National Academy of Sciences 101 (8), 2375–2380.